Heat Transfer Research 45(2), 145–169 (2014)

FREE CONVECTION IN RECTANGULAR ENCLOSURES CONTAINING NANOFLUID WITH NANOPARTICLES OF VARIOUS DIAMETERS

Saeid Jani,[1] Mostafa Mahmoodi,[2,] Meysam Amini[3] & Mohammad Akbari[4]*

[1]*Department of Mechanical Engineering, Golpayegan College of Engineering, Golpayegan, Iran*

[2]*Mechanical Engineering Department, Amirkabir University of Technology, Tehran, Iran*

[3]*Department of Mechanical Engineering, University of Kashan, Kashan, Iran*

[4]*Department of Mechanical Engineering, Najafabad Branch, Islamic Azad University, Isfahan, Iran*

[*]Address all correspondence to Mostafa Mahmoodi
E-mail: mmahmoodi46@gmail.com

Free convection heat transfer in rectangular enclosures filled with Al_2O_3–water nanofluid is investigated numerically, and the effects of suspended nanoparticles of different diameters are considered. The governing equations in terms of primitive variables are discretized numerically using the finite volume method and SIMPLER algorithm. The results were obtained for width range of the Rayleigh number, nanoparticles volume fraction and aspect ratio of cavity. Also nanoparticles with two different diameters, namely 36 nm and 47 nm have been chosen. The obtained results showed that for the square enclosure utilizing the suspended nanoparticles with both considered diameters the rate of heat transfer increased only at $Ra = 10^3$ that conduction dominated the heat transfer process, while at other Rayleigh numbers, a deterioration on average Nusselt number was observed.

KEY WORDS: *numerical simulation, finite volume method, nanofluid, heat transfer enhancement*

1. INTRODUCTION

Buoyancy-driven heat transfer is an important phenomenon because of its wide usage in engineering systems such as cooling of electronic devices, heat exchangers, building ventilation, insulation of reactors, and solar collectors (Ostrach, 1988). In

NOMENCLATURE

AR	aspect ratio, H/W	W	width of the cavity, m
c_p	heat capacitance of nanoparticles, $J \cdot kg^{-1} \cdot K^{-1}$	x, y	dimensional Cartesian coordinates, m
		X, Y	dimensionless Cartesian coordinates
d	diameter, m	**Greek symbols**	
g	gravitational acceleration, $m \cdot s^{-2}$	α	thermal diffusivity, $m^2 \cdot s^{-1}$
h	heat transfer coefficient, $W \cdot m^{-2} \cdot K$	β	thermal expansion coefficient, K^{-1}
H	height of the cavity, m	θ	dimensionless temperature
k	thermal conductivity, $W \cdot m^{-1} \cdot K^{-1}$	μ	dynamic viscosity, $kg \cdot m^{-1} \cdot s$
Nu	Nusselt number	ρ	density, $kg \cdot m^{-3}$
p	pressure, $N \cdot m^{-2}$	υ	kinematic viscosity, $m^2 \cdot s$
P	dimensionless pressure	φ	nanoparticle volume fraction
Pr	Prandtl number	ψ	stream function, $m^2 \cdot s^{-1}$
Ra	Rayleigh number	**Subscripts**	
T	dimensional temperature, K	c	cold
u, v	dimensional velocity component	f	fluid
	in x and y directions, $m \cdot s^{-1}$	h	hot
U, V	dimensionless velocities	nf	nanofluid
	in X and Y directions	p	nanoparticle

these systems, the intention of designers is the achievement of smaller dimensions and higher efficiency which is limited due to the low thermal conductivity of the fluid such as oil and water. Enhancement in the heat transfer rate and thermal conductivity of liquids was achieved previously by adding micro-sized particles to a base fluid (Maxwell, 1904). But rapid sedimentation resulted in a high pressure drop. In spite of this, a small amount of dispersed nano-sized particles is stably suspended and enhances the thermal properties of a base fluid. The mixture of suspended nanoparticles in the base fluid is named nanofluid. In comparison with microscale particles, nanoparticles cause better enhancement of the thermal properties of base fluid such as the thermal conductivity because of having bigger surface area (Godson et al., 2010).

The nanofluid can be used in natural convection cooling of cavities. In the work on free convection of nanofluid in differentially heated rectangular enclosures made by Khanafer et al. (2003) it was reported on increase in the rate of heat transfer with the volume fraction of nanoparticles. Oztop and Abu-nada (2008) studied free convection

in a nanofluid-filled square enclosure with a cold vertical wall and a heater located on the other vertical wall, using the finite volume method. They considered the effect of Rayleigh number, heater size, location, and volume fraction of the nanoparticles. Abu-nada and Oztop (2009) investigated numerically the effect of inclination angle of a nanofluid-filled square cavity on free convection fluid flow and heat transfer inside it. They utilized Cu–water nanofluid and found that the effect of the concentration of nanoparticles on the Nusselt number is more pronounced at a low volume fraction than at a high one. Ogut (2009) studied numerically free convection fluid flow and heat transfer in an inclined square cavity. The top and bottom horizontal walls of the cavity were insulated, while the right vertical wall was kept at a constant temperature T_c, and a heater was located on the left vertical wall. Numerical results of the study on periodic free convection heat transfer inside a nanofluid-filled square cavity were reported by Ghasemi and Aminossadati (2010). The geometry in their work was a square cavity with insulated top and bottom walls, cold right vertical wall and an oscillating heat flux heater on its left vertical wall. They observed periodic flow and temperature fields inside the cavity as a result of the oscillating heat flux. Sheikhzadeh and Mahmoodi (2011) investigated numerically free convection of Ag–water nanofluid in a square cavity with two or three pairs of hot and cold discrete elements on its side walls. Sheikhzadeh et al. (2011) conducted a numerical simulation to study free convection of Cu–water nanofluid inside a square cavity with partially thermally active side walls. Mahmoodi (2011) investigated numerically free convection of Cu–water nanofluid in L-shaped cavities. He found that the effect of the presence of nanoparticles on heat transfer enhancement is more apparent for narrow L-shaped cavities. Similar resuts were observed for free convection of nanofluids in C-shaped enclosures (Mahmoodi and Hashemi, 2012) and Γ-shaped cavities (Dehnavi and Rezvani, 2012). In all the above-mentioned papers, the Brinkman model (Brinkman, 1952) for viscosity and Maxwell model (Maxwell, 1904) for thermal conductivity were used, and an increasing Nusselt number with increasing volume fraction of nanoparticles was reported.

For all that, the results of experimental observations are different from the results of the numerical studies mentioned. Putra et al. (2003) carried out an experimental study on free convection of Al_2O_3–water nanofluid and argued that suspended nanoparticles in the base fluid deteriorated the heat transfer rate but they did not clarify the reasons for their result. Other experimental investigation was carried out by Wen and Ding (2004); they emphasized the reduction in the rate of natural convection heat transfer on utilizing nanofluid. One of the reasons for the difference between the numerical and experimental studies is the use of the Brinkman model to calculate the viscosity in numerical simulations. The Brinkman model for calculating the viscosity does not account for the size of nanoparticles and was derived for particles larger than nano-sized particles. The Brinkman model underestimates the value of viscosity (Nguyen et al., 2007b). Therefore to achieve more accurate numerical simulation of natural convection of nanofluids, it is appropri-

ate to use experimental correlations for viscosity and thermal conductivity. Other numerical studies that used more accurate relationships than the Brinkman model of viscosity, reported different results. Abu-nada et al. (2008) demonstrate numerically that the enhancement of heat transfer in free convection of nanofluid depends on the magnitude of the Rayleigh number. In fact, at the Rayleigh number lower than 10^4 an enhancement in the heat transfer rate with the volume fraction of nanoparticles is observed. Abu-nada et al. (2010) considered free convection of Al_2O_3–water and CuO–water nanofluids in a square cavity using volume fraction and temperature-dependent viscosity and thermal conductivity relationships numerically. The used viscosity and thermal conductivity relationships that were reported by Nguyen et al. (2007a) and Chon et al. (2005), respectively. They compared the results obtained by the mentioned model and the results of Brinkman and Maxwell models and showed that at high Rayleigh numbers, the heat transfer rate is sensitive to the viscosity model, while the thermal conductivity model has not any important influence on the heat transfer rate. Therefore the Maxwell thermal conductivity model can be used in numerical simulations dependably.

The Al_2O_3–water nanofluid is one of the nanofluids to which a large number of researches are devoted. A summary of derived models related to the Al_2O_3–water nanofluid can be found in Hwang et al. (2007). A polynomial curve fitting has been carried out on the experimental data reported by Wang et al. (1999). Also Nguyen et al. (2007b) obtained correlations for viscosity of the Al_2O_3–water nanofluid with two different nanoparticle diameters. The correlations are related to spherical nanoparticles with 36-nm and 47-nm diameters.

In the present study, free convection of the Al_2O_3–water nanofluid in a rectangular enclosure with varying aspect ratio is considered. To estimate the viscosity, the correlations reported by Nguyen et al. (2007b) are used. As mentioned before, this model had been derived for two different diameters of nanoparticles: 36 nm and 47 nm. Therefore the aim of this research is to considere the effect of the diameter of nanoparticles on free convection fluid flow and heat transfer. The isotherms, stream functions, and average Nusselt number are employed in the present paper to visualize the heat transport process.

2. PROBLEM DEFINITION

A schematic view of a differentially heated cavity considered in this study is displayed in Fig. 1. The width and height of the enclosure are W and H, respectively. The aspect ratio of the enclosure is defined as $AR = H/W$. The left wall is maintained at a constant uniform temperature T_h, while the right wall is maintained at a relatively low temperature T_c. The cavity is filled with Al_2O_3–water nanofluid. The thermophysical properties of the base fluid and the Al_2O_3 nanoparticles are listed in Table 1. The range of the Rayleigh number, aspect ratio, and the volume fraction of the nanoparticles are

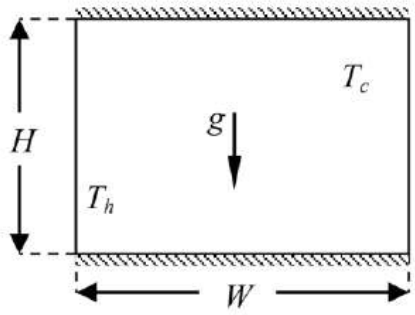

FIG. 1: A schematic view of the enclosure considered in the present paper

TABLE 1: Thermophysical properties of the base fluid and Al_2O_3 nanoparticles

	Water	Al_2O_3
ρ (kg·m^{-3})	997.1	3970
c_p (J·kg^{-1}·K^{-1})	4179	765
k (W·m^{-1}·K^{-1})	0.613	25
β (K^{-1})	$21\cdot10^{-5}$	$0.85\cdot10^{-5}$

10^3 to 10^6, 0.25 to 4, and 0 to 0.04, respectively. Also the spherical nanoparticles of diameters 36 nm and 47 nm are employed.

3. MATHEMATICAL FORMULATION

The nanofluid in the present study is Newtonian, incompressible, and the fluid flow is considered to be laminar. It is assumed that both nanoparticles and base fluid are in thermal equilibrium and there is no slip between them. The thermophysical properties of the nanofluid are considered to be constant with the exception of density which varies according to the Boussinesq approximation (Bejan, 1984).

The continuity, momentum, and energy equations are written in dimensional form as

$$\frac{\partial u}{\partial x} + \frac{\partial v}{\partial y} = 0\,, \tag{1}$$

$$u\,\frac{\partial u}{\partial x} + v\,\frac{\partial u}{\partial y} = -\frac{1}{\rho_{nf}}\,\frac{\partial p}{\partial x} + \frac{\mu_{nf}}{\rho_{nf}}\left(\frac{\partial^2 u}{\partial x^2} + \frac{\partial^2 u}{\partial y^2}\right), \tag{2}$$

$$u\,\frac{\partial v}{\partial x} + v\,\frac{\partial v}{\partial y} = -\frac{1}{\rho_{nf}}\,\frac{\partial p}{\partial y} + \frac{\mu_{nf}}{\rho_{nf}}\left(\frac{\partial^2 v}{\partial x^2} + \frac{\partial^2 v}{\partial y^2}\right) + \frac{(\rho\beta)_{nf}\; g\,(T - T_c)}{\rho_{nf}}\,, \tag{3}$$

$$u\,\frac{\partial T}{\partial x} + v\,\frac{\partial T}{\partial y} = \alpha_{nf}\left(\frac{\partial^2 T}{\partial x^2} + \frac{\partial^2 T}{\partial y^2}\right). \tag{4}$$

As mentioned before, in some papers the Brinkman model is used for calculation of viscosity. It is recently found that the Brinkman model underestimates the viscosity (Nguyen et al., 2007b). The Brinkman model is

$$\frac{\mu_{nf}}{\mu_f} = \frac{1}{(1-\varphi)^{2.5}}. \tag{5}$$

In the present study, the correlations reported by Nguyen et al. (2007b) are used to estimate the effective viscosity of nanofluid. They proposed the following correlations for the particles 47 nm and 36 nm in size, respectively:

$$\frac{\mu_{nf}}{\mu_f} = 0.904\, e^{0.1483\varphi}, \tag{6}$$

$$\frac{\mu_{nf}}{\mu_f} = 1 + 0.025\,\varphi + 0.015\,\varphi^2. \tag{7}$$

In Eqs. (5) and (6), φ belongs to percentage terms. The viscosities estimated by Eqs. (5), (6), and (7) are shown in Fig. 2. Also the viscosity correlation obtained by Corcione (2011) is shown in the figure. The correlation proposed by Corcione (2011) was obtained by a curve fitting on a large number of experimental data for different nanofluids. It is evident that the viscosity estimated by the Brinkman model is lower than those given by other models. Moreover, the nanofluid with nanoparticles of 47 nm in diameter has higher viscosity than that with nanoparticles of 36 nm in diameter. A comparison with the results obtained by the correlation proposed by Corcione (2011) shows the accuracy of the models and experiments of Nguyen et al. (2007b).

The effective density, heat capacitance, and thermal expansion coefficient of a nanofluid are (Khanafer et al., 2003):

$$\rho_{nf} = (1-\varphi)\,\rho_f + \varphi\,\rho_p, \tag{8}$$

$$(\rho c_p)_{nf} = (1-\varphi)\,(\rho c_p)_f + \varphi\,(\rho c_p)_p, \tag{9}$$

$$(\rho\beta)_{nf} = (1-\varphi)\,(\rho\beta)_f + \varphi\,(\rho\beta)_p. \tag{10}$$

The thermal conductivity of a nanofluid with spherical nanoparticles is calculated according to Maxwell (1904) as

$$k_{nf} = k_f\left[\frac{(k_p + 2k_f) - 2\varphi\,(k_f - k_p)}{(k_p + 2k_f) + \varphi\,(k_f - k_p)}\right]. \tag{11}$$

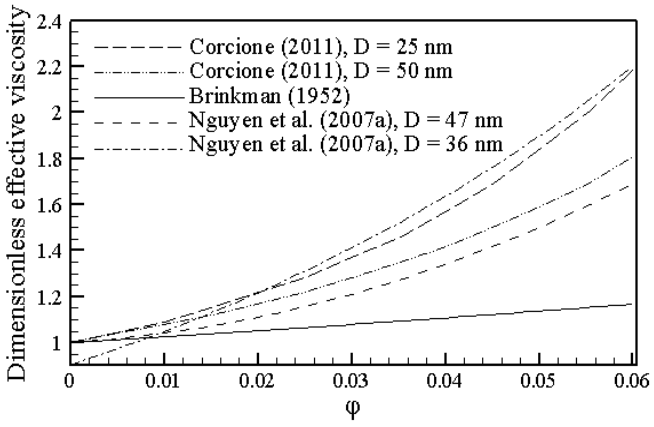

FIG. 2: Calculated dimensionless viscosity of the Al_2O_3–water nanofluid with different correlations

Using the following dimensionless parameters, the above equations can be converted to a nondimensional form:

$$X = \frac{x}{H}\,,\quad Y = \frac{y}{H}\,,\quad U = \frac{uH}{\alpha_f}\,,\quad V = \frac{vH}{\alpha_f}\,,\quad P = \frac{pH^2}{\rho_{nf}\alpha_f^2}\,,\quad \theta = \frac{T - T_c}{T_h - T_c}\,,$$
$$Ra = \frac{g\beta_f H^3 \Delta T}{\upsilon_f \alpha_f}\,,\quad Pr = \frac{\upsilon_f}{\alpha_f}\,. \tag{12}$$

where Ra and Pr are the Rayleigh and Prandtl number, respectively. The dimensional forms of the governing equations are

$$\frac{\partial U}{\partial X} + \frac{\partial V}{\partial Y} = 0\,, \tag{13}$$

$$U\,\frac{\partial U}{\partial X} + V\,\frac{\partial U}{\partial Y} = -\,\frac{\partial P}{\partial X} + \frac{\upsilon_{nf}}{\alpha_f}\left(\frac{\partial^2 U}{\partial X^2} + \frac{\partial^2 U}{\partial Y^2}\right), \tag{14}$$

$$U\,\frac{\partial V}{\partial X} + V\,\frac{\partial V}{\partial Y} = -\,\frac{\partial P}{\partial Y} + \frac{\upsilon_{nf}}{\alpha_f}\left(\frac{\partial^2 V}{\partial X^2} + \frac{\partial^2 V}{\partial Y^2}\right) + \frac{(\rho\beta)_{nf}}{\rho_{nf}\beta_f}\,Ra\;Pr\;\theta\,, \tag{15}$$

$$U\,\frac{\partial \theta}{\partial X} + V\,\frac{\partial \theta}{\partial Y} = \frac{\alpha_{nf}}{\alpha_f}\left(\frac{\partial^2 \theta}{\partial X^2} + \frac{\partial^2 \theta}{\partial Y^2}\right). \tag{16}$$

The initial and the boundary conditions for the present study are

$$0 \le X \le 1\,,\qquad Y = 0 \;\rightarrow U = V = \partial\theta/\partial Y = 0\,,$$

$$0 \le X \le 1, \qquad Y = 1 \rightarrow U = V = \partial\theta/\partial Y = 0,$$

$$X = 0, \qquad 0 \le Y \le 1 \rightarrow U = V = 0, \qquad \theta = 1, \tag{17}$$

$$X = 1, \qquad 0 \le Y \le 1 \rightarrow U = V = 0, \qquad \theta = 0.$$

The local Nusselt number is calculated as follows (Mahmoodi, 2011):

$$Nu_{local} = \frac{hH}{k_f} = -\left(\frac{k_{nf}}{k_f}\right)\frac{\partial\theta}{\partial X}. \tag{18}$$

The average Nusselt number is calculated from

$$Nu = \int_0^1 Nu(y)dY. \tag{19}$$

The normalized average Nusselt number is defined as the ratio of the average Nusselt number of nanofluid to the average Nusselt number of pure fluid:

$$Nu^* = \frac{Nu(\varphi)}{Nu\,(\varphi = 0)}. \tag{20}$$

The normalized average Nusselt number is used to measure the heat transfer enhancement utilizing nanofluid compared to a base fluid.

4. NUMERICAL METHOD

The nonlinear governing (continuity, momentum, and energy) equations written in terms of the primitive variables are discretized using the finite-volume approach given by Patankar (1980). The coupling of pressure and velocity is done by the SIMPLER algorithm. The diffusion terms in the momentum and energy equations are approximated by a second order central difference scheme, while a hybrid scheme, which is a combination of central difference and upwind schemes, is employed to discretize the convection terms. The set of discretized equations are solved by the TDMA line-by-line method (Hoffman, 2001) that yields the value of velocity, pressure, and temperature at the nodal points.

To grid test the study, a differentially heated square cavity filled with Al_2O_3–water nanofluid with nanoparticles with 0.04 and 36 nm in diameter at $Ra = 10^6$ is considered. Four different uniform grid sizes, namely, 21 × 21, 41 × 41, 81 × 81, and 161 × 161, are used and the average Nusselt number along the hot vertical wall of the cavity is obtained for each case. As shown in Table 2, the results of the 81 × 81 and 161 × 161 grid sizes are equal, so the 81 × 81 grid size has been chosen. A similar type of the grid test study has been carried out for other aspect ratios, but is not reported here.

In order to validate the obtained numerical code, we considered the problem of free convection in a square cavity with a heat source and sink on its left and right wall, re-

TABLE 2: Comparison of average Nusselt number for different grid sizes

Grid size	21 × 21	41 × 41	81 × 81	161 × 161
Nu	7.311	8.511	8.872	8.873

TABLE 3: The average Nusselt number of the hot walls for the second test case, comparison of the present results with the results of Sheikhzadeh et al. (2011)

	Present study	Sheikhzadeh et al. (2011)
$Ra = 10^3$	2.218	2.228
$Ra = 10^4$	3.715	3.709
$Ra = 10^5$	7.221	7.160
$Ra = 10^6$	12.905	12.881

spectively, and filled with Cu–water nanofluid with $\varphi = 0.1$ at different Rayleigh numbers. Table 3 shows a comparison between the average Nusselt numbers obtained by the present numerical simulation with those presented by Sheikhzadeh et al. (2011). As can be seen from the table, very good agreement exists between the results of the current simulation with those of other investigators.

5. RESULTS AND DISCUSSION

In this section, numerical results on free convection heat transfer of Al_2O_3–water nanofluid inside differentially heated rectangular cavities are presented. The results were obtained for the Rayleigh number ranging from 10^3 to 10^6, the volume fraction of the nanoparticles varying from 0 to 0.04, and the aspect ratio of cavity ranging from 0.25 to 4. The results are presented in terms of streamlines, isotherms, average Nusselt number, and normalized Nusselt number.

It should be noted that the suspended nanoparticles in the base fluid have two opposing effects on the rate of heat transfer. In free convection flow, dispersed nanoparticles in the base fluid will make the nanofluid more viscous. The increasing viscosity reduces the fluid flow velocity and strength that decreases the rate of heat transfer. On the other hand, nanofluid has a higher thermal conductivity than the base fluid that increases the rate of heat transfer. Therefore if the heat transfer enhancement due to the presence of high thermal conductivity outranks deterioration of heat transfer because of the high level of viscosity, the total rate of heat transfer increases, otherwise it decreases.

Figure 3 illustrates variations of the vertical velocity component along the horizontal mid-line of the cavity with $AR = 1$ for pure fluid and nanofluid with $\varphi = 0.04$ and

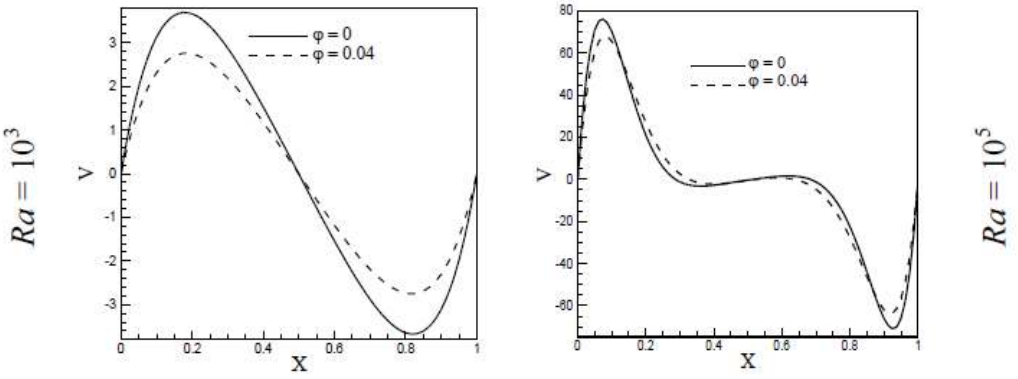

FIG. 3: Variation of vertical velocity component along the horizontal mid-line of the cavity with volume fraction of nanoparticles (AR = 1, D = 36 nm)

D = 36 nm at $Ra = 10^3$ and 10^5. As shown in Fig. 3, the vertical velocity component decreases with increase in the nanoparticles volume fraction. Moreover, it is evident that the reduction in the vertical velocity at low Rayleigh numbers is greater than that at high Rayleigh numbers. Also it is shown in Fig. 3b that on increase in the volume fraction of the nanoparticles, the vertical velocity component adjacent to the vertical walls decreases, while it increases in the middle region of the cavity, that is to say, the thickness of the velocity boundary layer adjacent to the vertical wall increases with increase in the volume fraction of nanoparticles. It is the undesirable effect of nanoparticles in the base fluid which reduces the rate of heat transfer.

For a better understanding of the effect of φ on flow pattern in Fig. 4, the streamlines inside the square cavity for nanofluid with nanoparticles of 47 nm and 36 nm in diameter are compared with those of pure fluid at $Ra = 10^5$. From this figure, it is seen that with increase in the volume fraction of the nanoparticles and subsequent increase in viscosity, the difference between the results for the nanofluid and pure fluid and also the difference between the results for the nanofluid with D = 47 nm and 36 nm increase. With increase in the volume fraction of the nanoparticles, the condensation of the streamlines in the vicinity of the side wall decreases. This decrease is more apparent for the cavity with the nanoparticles having D = 36 nm. Figure 5 shows the vertical velocity component along the horizontal mid-line of the cavity for two different nanoparticle diameters at $Ra = 10^6$. It is evident that the velocity of nanoparticles 47 nm in diameter is less than that with 36 nm diameter. Therefore it can be concluded that the nanofluid with larger diameters of nanoparticles has a minor effect on the velocity domain.

Figure 6 illustrates isotherms inside the square cavity for nanofluids with nanoparticles having D = 36 nm and 47 nm at $Ra = 10^5$. It is evident that with increase in the volume fraction of the nanoparticles the agglomeration of isotherms adjacent to

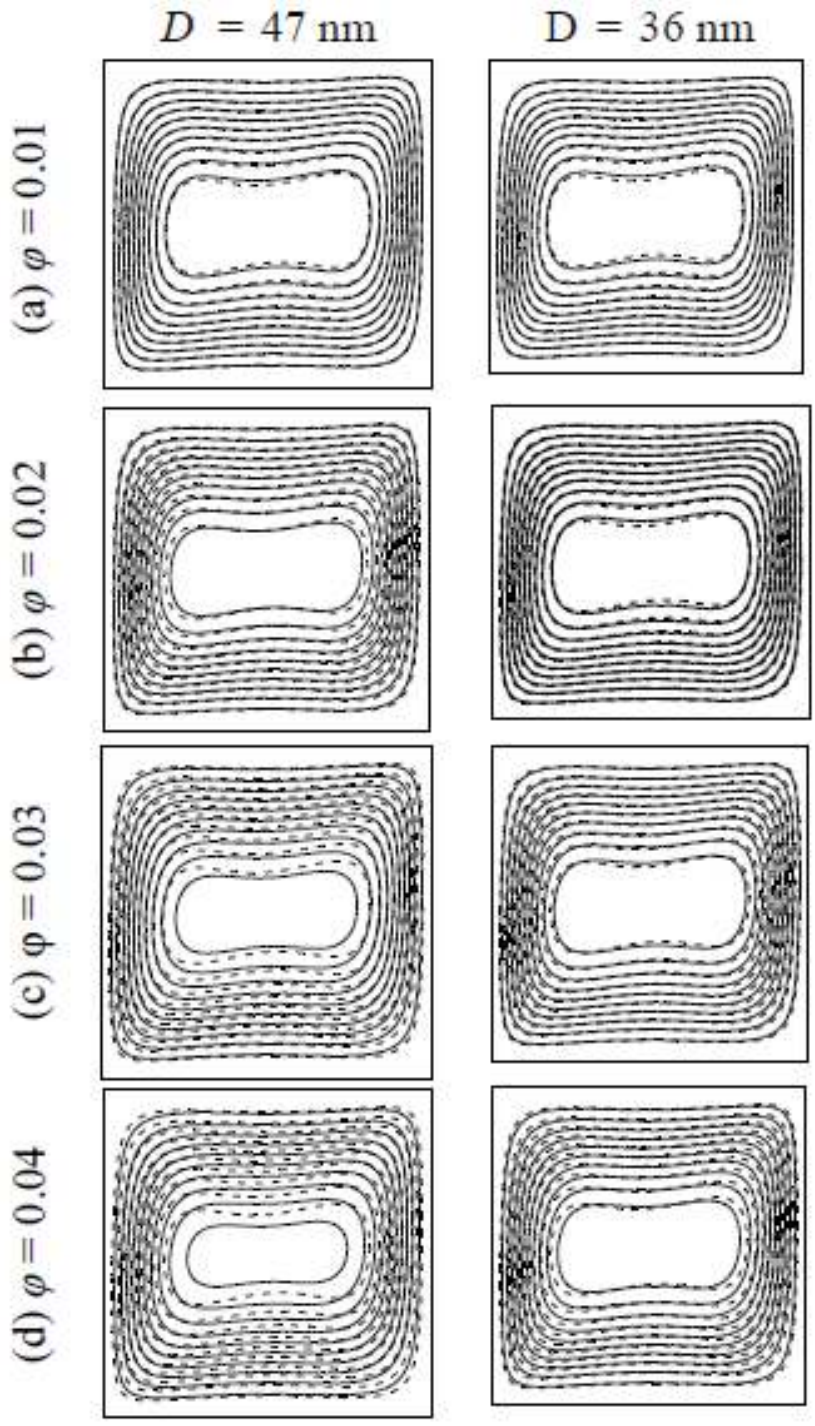

FIG. 4: Streamlines for nanofluid with φ = 0.04 (solid lines) and pure fluid (dashed lines) at $Ra = 10^5$

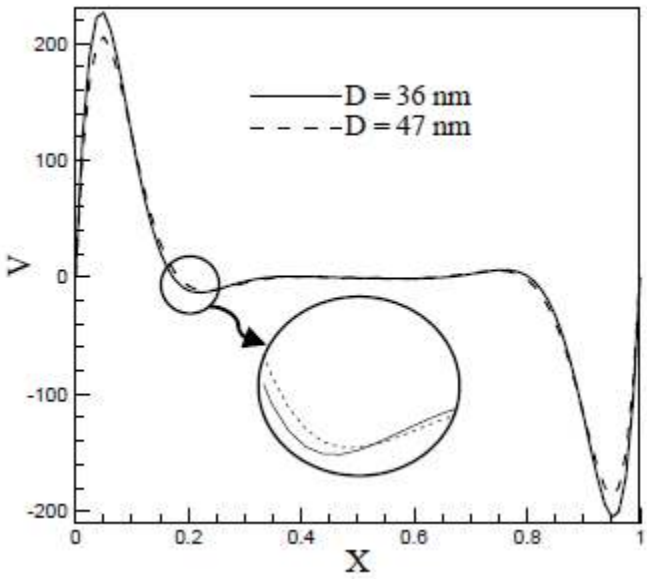

FIG. 5: Comparison between vertical velocity components of nanofluid with different diameters of nanoparticles

vertical walls is reduced. The difference between the results for the nanoparticles with D = 47 nm and 36 nm is more apparent at $\varphi = 0.04$. Also it is found that the existence of the nanoparticles in the base fluid does not have a considerable effect on the thermal stratified region in the middle of the cavity.

Figure 7 illustrates the effect of nanofluid with different diameters of nanoparticles on the average Nusselt number for the hot wall of the square cavity. It is evident that only at $Ra = 10^3$, suspended nanoparticles increase the Nusselt number for two different nanoparticle diameters. At $Ra = 10^3$, conduction dominates over the heat transfer and the high thermal conductivity of the nanofluid enhances the rate of heat transfer. However, at higher Rayleigh numbers, convection dominates over the heat transfer, and the high viscosity of nanofluid reduces the flow velocity and causes a reduction in the heat transfer rate that the high thermal conductivity of nanofluid cannot retrieve this reduction. The reduction of the flow strength by increasing the volume fraction of nanoparticles is carried out at $Ra = 10^3$ too. However, as mentioned before, at $Ra = 10^3$ the heat transfer is dominated by conduction, and the high thermal conductivity of nanofluids is more efficient.

Figures 8 and 9 show variation of normalized average Nusselt number with the volume fraction of nanoparticles for different aspect ratios and for D = 36 nm and 47 nm, respectively. Figures 8a and 9a are related to the cavity with $AR = 0.25$. For $Ra = 10^3$, the values of Nu^* are greater than unity. Therefore for all ranges of nanoparticle volume fraction, the rate of heat transfer is higher than that for the base fluid at $Ra = 10^3$. With

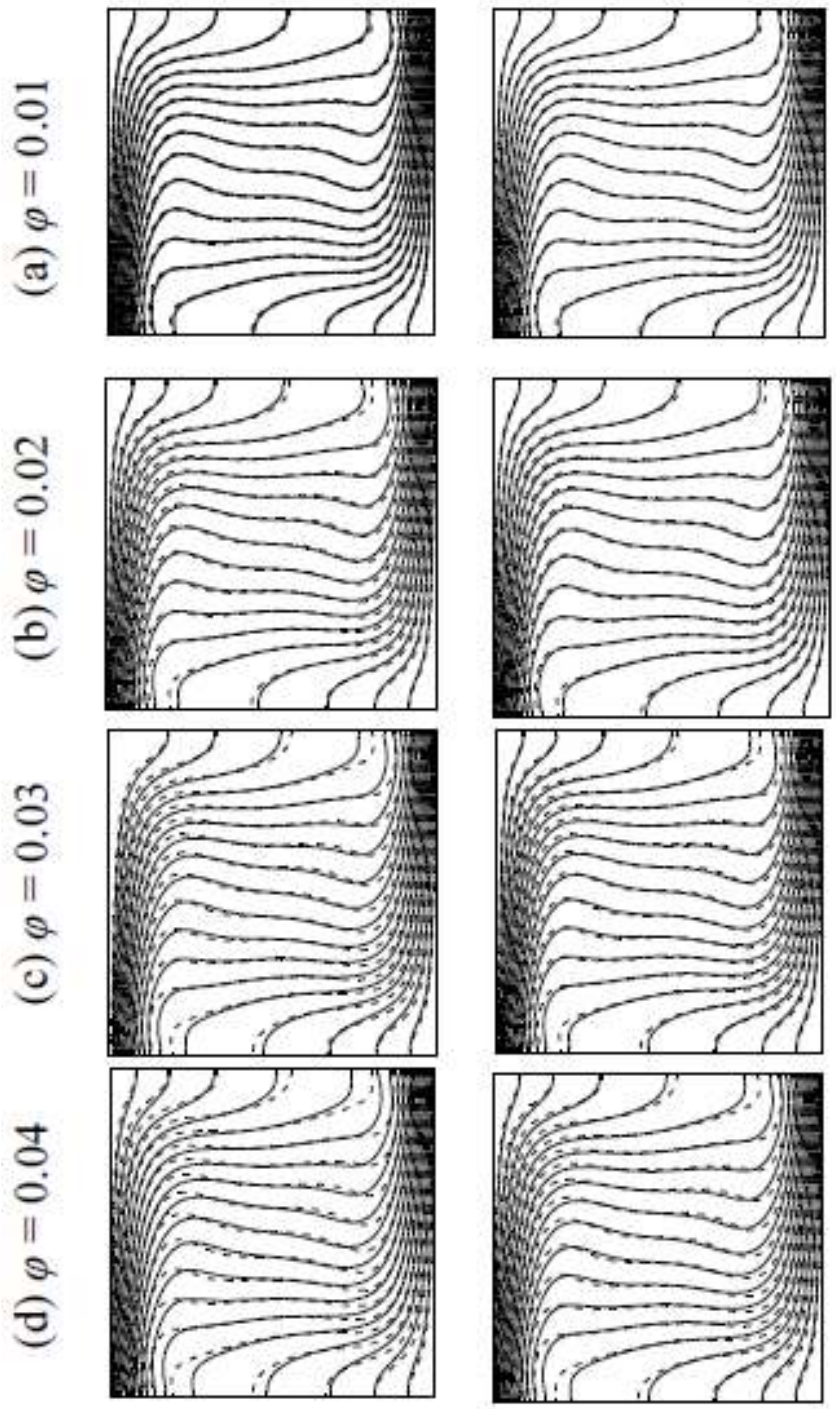

FIG. 6: Isotherms for nanofluid with φ = 0.04 (solid lines) and pure fluid (dashed lines) at $Ra = 10^5$

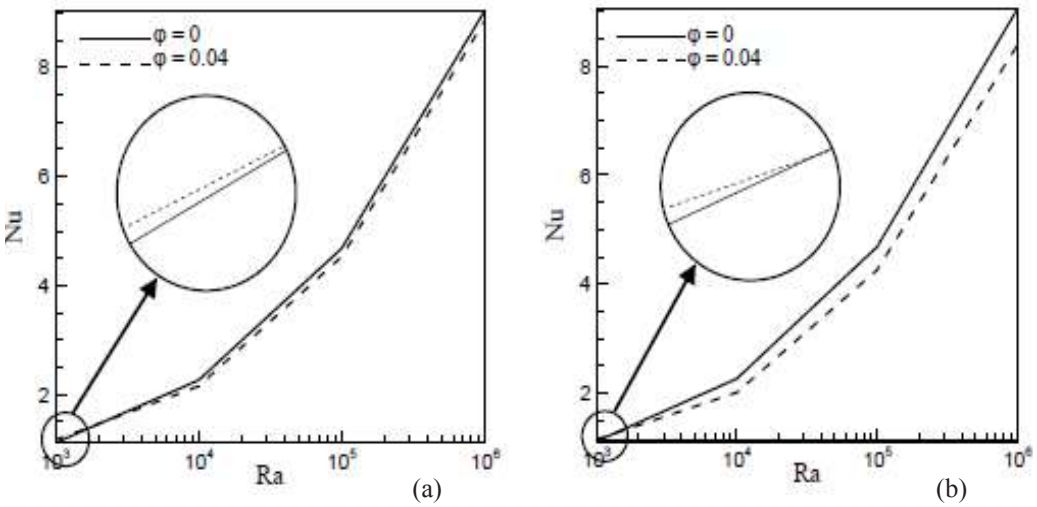

FIG. 7: Variation of the average Nusselt number of the hot wall of the square cavity for the nanofluid with nanoparticle diameter equal to (a) D = 36 nm, (b) D = 47 nm

increase in the Rayleigh number, an intense reduction in the normalized average Nusselt number is evident, and higher rate of decrease in the normalized average Nusselt number by increase in the volume fraction of nanoparticles occurs at $Ra = 10^4$. At $Ra = 10^4$, the contributions of conduction and convection are comparable and the convection is not very appreciable. At this Rayleigh number the decrease in the heat transfer rate via high viscosity of nanofluid is larger than the increase in the heat transfer rate via high thermal conductivity of nanofluid, hence the net rate of heat transfer decreases with increase in the nanoparticle volume fraction. At $Ra = 10^5$ and 10^6 the Nu^* number is higher than that at $Ra = 10^4$; however, it is lower than unity yet and nanoparticles increase the rate of heat transfer only at $Ra = 10^3$.

Figures 8b and 9b are related to the cavity with AR = 1. The behavior similar to AR = 0.25 is evident for the case of AR = 1. Figures 8c and 9c contain the result of AR = 4. For the high aspect ratio cavity, conduction dominates over the heat transfer at higher value of Rayleigh number compared to the cavity with a low aspect ratio (Bejan, 1984). Therefore for AR = 4, nanoparticles increase the heat transfer rate at $Ra = 10^4$ too. Variation of Nu^* at $Ra = 10^4$ has a trend similar to that at $Ra = 10^3$. In the case of AR = 4, the normalized average Nusselt numbers related to $Ra = 10^5$ are higher than those related to $Ra = 10^6$. It is inverse in comparison with the case of AR = 1 and 0.25. For $Ra = 10^5$ and 10^6 in Fig. 9c, fluctuation of Nu^* is observed; a similar trend was obtained by Abu-nada et al. (2010), and they clarified it thoroughly.

Figure 10 depicts the effect of AR on Nu^* for nanoparticles with D = 36 nm. As shown in Fig. 10a, the larger aspect ratio at $Ra = 10^3$ causes greater enhancement of Nu^*. Figures 10b and 10c are related to the cases of $Ra = 10^4$ and 10^5, respectively. It

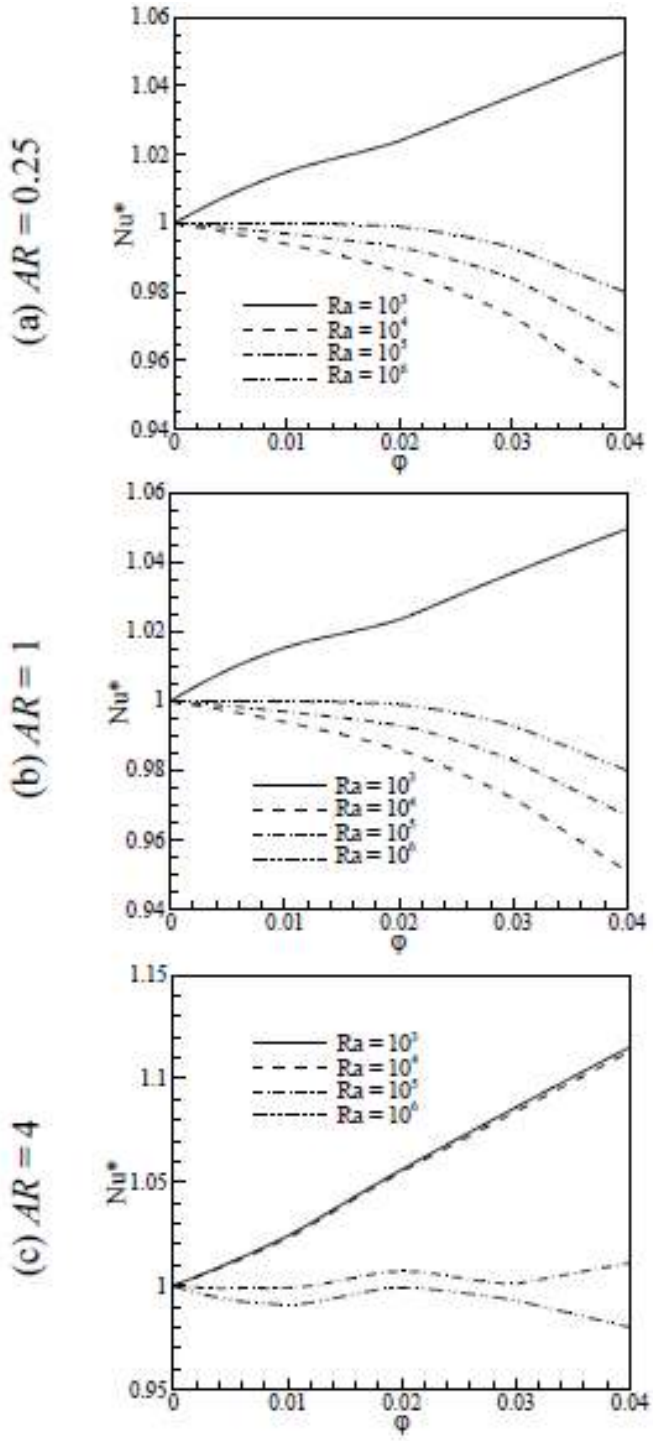

FIG. 8: Normalized average Nusselt number vs. nanoparticles volume fraction for D = 36 nm

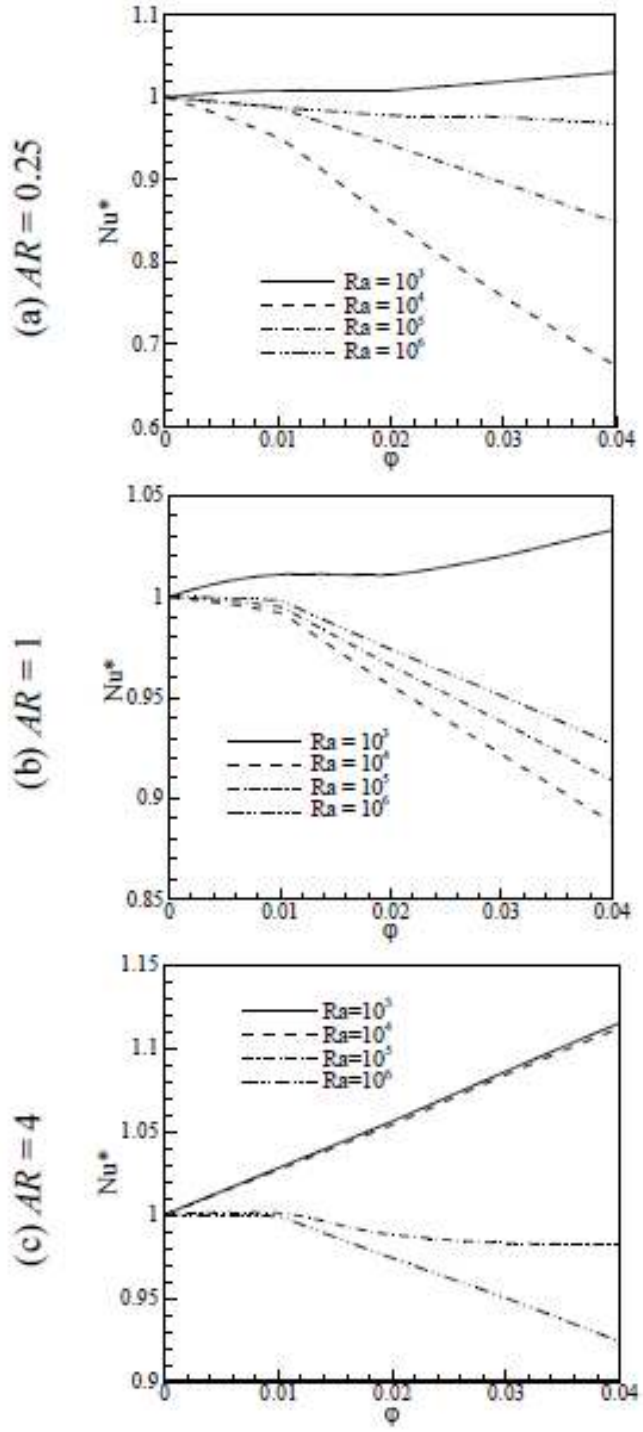

FIG. 9: Normalized average Nusselt number vs. nanoparticles volume fraction for D = 47 nm

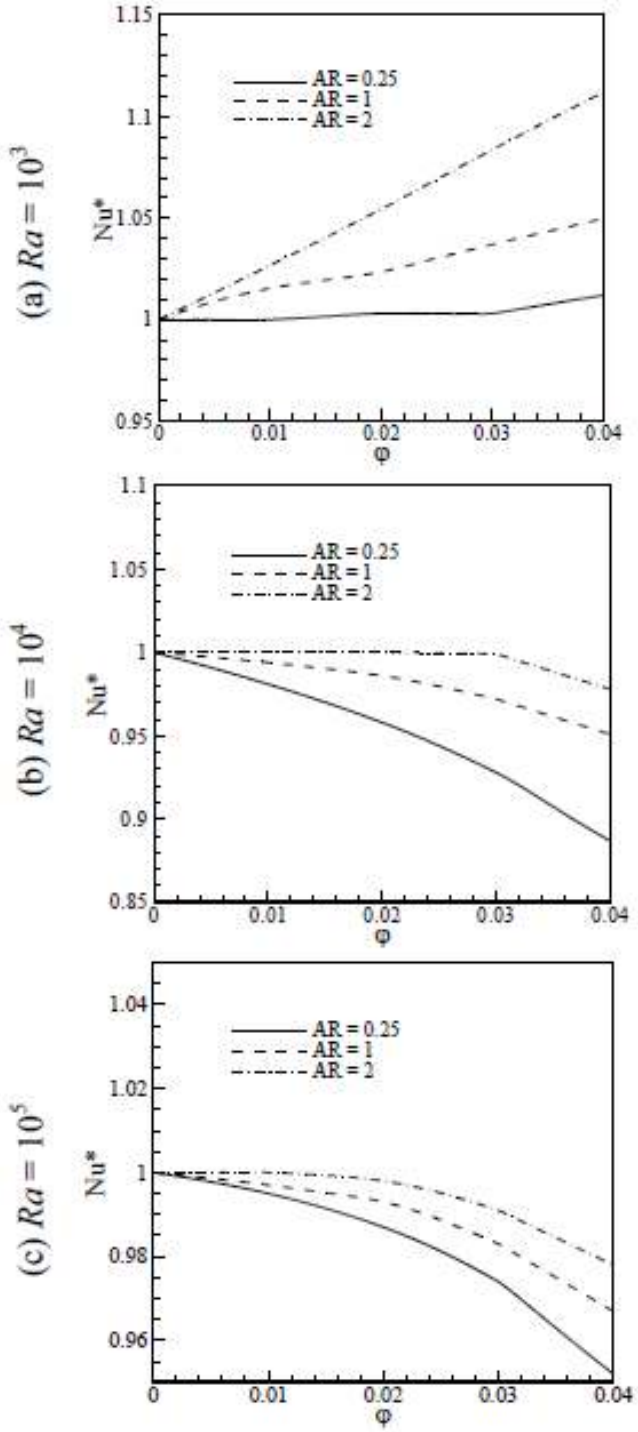

FIG. 10: Normalized average Nusselt number vs. nanoparticles volume fraction for D = 36 nm

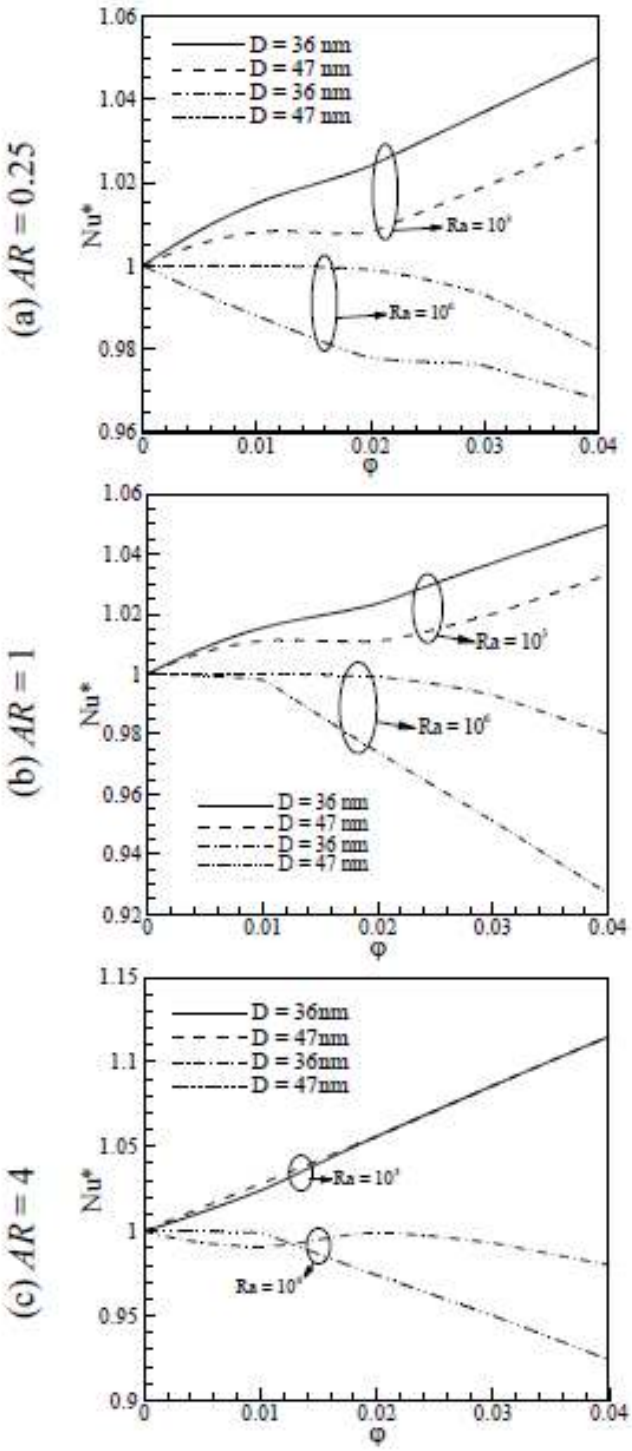

FIG. 11: Effect of various nanoparticle diameters on the normalized average Nusselt number

is evident that cavities with high aspect ratios cause less deterioration of the normalized average Nusselt number compared to the cavities with low aspect ratio.

The effect of different nanoparticle diameters on the normalized average Nusselt number is shown in Fig. 8. Figures 11a,b,c show the result obtained for $AR = 0.25$, 1, and 4, respectively. For cavities with $AR = 0.25$ and 1, the nanofluid with D = 47 nm causes smaller enhancement of Nu^* at $Ra = 10^3$ and more deterioration of Nu^* at $Ra = 10^6$ compared to the nanofluid with nanoparticles of 36 nm in diameter. This is due to the higher viscosity of nanofluid with nanoparticles of 47 nm in diameter than that of nanoparticles with 36 nm in diameter. With increase in the aspect ratio, the difference between the results of nanofluids with different diameters of nanoparticles at $Ra = 10^3$ decreases, since at $AR = 4$ the difference decreases approximately. However, at $Ra = 10^4$ the difference still exists.

6. CONCLUSIONS

In this study, the free-convection heat transfer in rectangular enclosures filled with Al_2O_3–water nanofluid was investigated numerically using the finite volume method. A parametric study was performed, and the effects of the Rayleigh number, the volume fraction of the nanoparticles, the diameter of the spherical nanoparticles, and the aspect ratio of the cavity on the fluid flow and heat transfer were investigated and the following results were obtained:

Suspended nanoparticles of larger diameter provide nanofluids of higher viscosity.

For a cavity with $AR = 1$ and two different diameters of nanoparticles, only at $Ra = 10^3$, conduction dominates over heat transfer, suspended nanoparticles increase the rate of heat transfer and at other values of Rayleigh numbers, high viscosity of nanofluid reduces flow strength and the rate of heat transfer.

For a cavity with $AR = 4$, at $Ra = 10^4$, increase in the volume fraction of nanoparticles increases the rate of heat transfer similarly to $Ra = 10^3$.

Nanofluid with larger nanoparticles has less influence on heat transfer enhancement at $Ra = 10^3$ and has a higher effect on heat transfer deterioration at $Ra > 10^3$ than the nanofluid with a smaller diameter of nanoparticles.

For a cavity with $AR = 4$ and at $Ra = 10^3$, a similar trend in heat transfer enhancement utilizing nanofluid with different diameters of nanoparticles is observed; this does not occur at other aspect ratios.

REFERENCES

Abu-nada, E. and Oztop, H., Effect of inclination angle on natural convection in enclosures filled with Cu–water nanofluid, *Int. J. Heat Fluid Flow*, vol. 30, pp. 669–678, 2009.

Abu-nada, E., Masoud, Z., and Hijazi, A., Natural convection heat transfer enhancement in concentric annuli using nanofluids, *Int. Commun. Heat Mass Transfer*, vol. 35, no. 5, pp. 657–665, 2008.

Abu-nada, E., Masoud, Z., Oztop, H., and Campo, A., Effect of nanofluid variable properties on natural convection in enclosures, *Int. J. Thermal Sci*., vol. 49, no. 3, pp. 479–491, 2010.

Bejan, A., *Convection Heat Transfer*, New York: John Wiley and Sons, 1984.

Brinkman, H. C., The viscosity of concentrated suspensions and solution, *J. Chem. Phys*., vol. 20, pp. 571–581, 1952.

Chon, C. H., Kihm, K. D., Lee, S. P., and Choi, S. U. S., Empirical correlation finding the role of temperature and particle size for nanofluid (Al_2O_3) thermal conductivity enhancement, *Appl. Phys. Lett*., vol. 87, 153107, 2005.

Corcione, M., Empirical correlating equations for predicting the effective thermal conductivity and dynamic viscosity of nanofluids, *Energy Conversion Management*, vol. 52, pp. 789–793, 2011.

Dehnavi, R. and Rezvani, A., Numerical investigation of natural convection heat transfer of nanofluids in a Γ-shaped cavity, *Superlattices Microstructures*, vol. 52, pp. 312–325, 2012.

Ghasemi B. and Aminossadati, S. M., Periodic natural convection in a nanofluid-filled enclosure with oscillating heat flux, *Int. J. Thermal Sci*., vol. 49, pp. 1–9, 2010.

Godson, L., Raja, B., Lal, D. M., and Wongwises, S., Enhancement of heat transfer using nanofluids — An overview, *Renewable Sustainable Energy Rev*., vol. 14, pp. 629–641, 2010.

Hoffman, J. D., *Numerical Methods for Engineers and Scientists*, Second ed., New York: Marcel Dekker Inc, 2001.

Hwang, K. S., Lee, J.-H., and Jang, S. P., Buoyancy-driven heat transfer of water-based Al_2O_3 nanofluids in a rectangular cavity, *Int. J. Heat Mass Transfer*, vol. 50, pp. 4003–4010, 2007.

Khanafer, K., Vafai, K., and Lightstone, M., Buoyancy-driven heat transfer enhancement in a two-dimensional enclosure utilizing nanofluid, *Int. J. Heat Mass Transfer*, vol. 46, pp. 3639–3653, 2003.

Mahmoodi, M. and Hashemi, S. M., Numerical study of natural convection of a nanofluid in C-shaped enclosures, *Int. J. Thermal Sci*., vol. 55, pp. 76–89, 2012.

Mahmoodi, M., Numerical simulation of free convection of a nanofluid in L-shaped cavities, *Int. J. Thermal Sci*., vol. 50, pp. 1731–1740, 2011.

Maxwell, J. C., *A Treatise on Electricity and Magnetism*, Second ed., Cambridge, UK: Oxford University Press, 1904.

Nguyen, C. T., Desgranges, F., Roy, G., Galanis, N., Mare, T., Boucher, S., and Minsta, H. A., Temperature and particle-size dependent viscosity data for water-based nanofluids — Hysteresis phenomenon, *J. Heat Fluid Flow*, vol. 28, pp. 1492–1506, 2007a.

Nguyen, C. T., Desgranges, F., Roy, G., Galanis, N., Mare, T., Boucher, S., and Minsta, H. A., Viscosity data for Al_2O_3-water nanofluid – hysteresis: is heat transfer enhancement using nanofluids reliable? *Int. J. Thermal Sci*., vol. 47, pp. 103–111, 2007b.

Ogut, E. B., Natural convection of water-based nanofluids in an inclined enclosure with a heat source, *Int. J. Thermal Sci*., vol. 48, no. 11, pp. 2063–2073, 2009.

Ostrach, S., Natural convection in enclosures, *ASME J. Heat Transfer*, vol. 110, pp. 1175–1190, 1988.

Oztop, H. and Abu-nada, E., Numerical study of natural convection in partially heated rectangular enclosures filled with nanofluids, *Int. J. Heat Fluid Flow*, vol. 29, pp. 1326–1336, 2008.

Patankar, S. V., *Numerical Heat Transfer and Fluid Flow*, Washington D.C.: Hemisphere Publishing Co., 1980.

Putra, N., Roetzel, W., and Das, S. K., Natural convection of nanofluids, *Heat Mass Transfer*, vol. 16, pp. 775–784, 2003.

Sheikhzadeh, G. A. and Mahmoodi, M., Numerical study of natural convection of nanofluid in a square cavity with hot and cold elements on its vertical walls (in Persian), *J. Comput. Meth. Eng*., vol. 30, pp. 79–96, 2011.

Sheikhzadeh, G. A., Arefmanesh, A., Kheirkhah, M. H., and Abdollahi, R., Natural convection of Cu–water nanofluid in a cavity with partially active side walls, *Eur. J. Mech. B/Fluids*, vol. 30, pp. 166–176, 2011.

Wang, X., Xu, X., and Choi, S. U. S., Thermal conductivity of nanoparticles–fluid mixture, *J. Thermophys. Heat Transfer*, vol. 13, no. 4, pp. 474–480, 1999.

Wen, D. and Ding, Y., Experimental investigation into convective heat transfer of nanofluids at the entrance region under laminar flow conditions, *Int. J. Heat Mass Transfer*, vol. 47, pp. 5181–5188, 2004.